Single-Molecule Measurements of Gold-Quenched Quantum Dots

Zoher Gueroui* and Albert Libchaber

Center for Studies in Physics and Biology, The Rockefeller University, 1230 York Avenue, New York, New York 10021, USA

(Received 5 April 2004; published 15 October 2004)

We report the study of the quenching of quantum dots (CdSe) by gold nanoparticles at the single-molecule level. Double-stranded DNA is used as a rigid spacer to tune the distance between the two nanoparticles. The width of the fluorescent intensity distribution, monitored at different interparticle distances, reflects both the nanoparticle heterogeneity and the fluorescence intermittency of the quantum dot. The fluorescence distribution emitted by single CdSe nanocrystals can easily be distinguished from the fluorescence of partially quenched CdSe. Our results show that the distance-dependence quenching is compatible with a Förster-type process.

DOI: 10.1103/PhysRevLett.93.166108 PACS numbers: 81.07.–b, 33.50.–j, 87.68.+z

Recently important progress has been made in the field of fluorescence detection of single molecules [1]. Such studies allow us to look beyond ensemble-average properties. For example, the fluorescence resonance energy transfer [2] provides a powerful method to measure the distance between two organic dyes [3]. Here, we study the energy transfer between two inorganic particles: a semiconductor nanocrystallite CdSe/ZnS quantum dot (Qdots) and a nanometer-sized gold (Au) cluster. Qdots and Au nanoparticles have gained considerable interest in the field of material science and biophotonics. Quantum dots can be viewed as artificial atoms intermediate between molecular and bulk forms of matter [4]. Given their photostability properties and their bright luminescence, tunable across the visible spectrum, they have proven to be useful as biological labels, sensors, laser, and single-photon sources [5–8]. They can now be synthesized at the size scale of biomolecules [9,10] and demonstrate attractive properties as inorganic structures to probe biological systems [11]. Colloidal gold nanoparticles have very interesting optical properties. Incident light can couple to the plasmon excitation of the metal and induce collective motion of the valence electrons [12]. These colloidal particles are also efficient fluorescent quenchers for organic dyes [13–15], and can be made as small as 1 nm in diameter. Two fundamental aspects combine to study this novel inorganic semiconductor (emitter)–metallic (quencher) pair. First, the description of the pair interaction as a function of the interparticle distance will help to unravel the physics underlying this process. Second, given this description numerous applications for biological science could be undertaken. With the measurement of the intermolecular distances between a single Qdot-Au pair, it will be possible to follow the conformational change of individual biomolecular assemblies. The Qdot we use is a core-shell CdSe/ZnS and the gold nanoparticle is a 1.4 nm gold cluster. To design this pair, we exploit the sequences-specific hybridization properties of DNA molecules, which offer simple and powerful building blocks to assemble objects at different scales [16]. Because of the 150 base pairs (bp) double-helix persistence length, the double-stranded-DNA (dsDNA) molecules we use to tune the distance between the Qdot and the Au nanoparticles are rigid [17,18]. We first measure the intensity distribution of individual Qdots and Qdots-dsDNA-Au complexes to measure the quenching efficiency transfer. The 1.4 nm Au nanoparticles quench the CdSe Qdots up to 83% when the interparticle distance is 5.9 nm. As a function of DNA length, the transfer satisfies a Förster process with a characteristic length of 7.5 nm [2].

Two steps are needed to form the hybrid system Qdot-DNA-Au. First, the Qdots are coupled to single stranded DNA (ssDNA) and the gold nanoparticles to ssDNA. In order to be biocompatible, Qdot nanocrystals were rendered water soluble after being encapsulated individually inside phospholipid micelles [19]. DNA oligonucleotides are acquired from commercially available synthetic oligonucleotides (Operon Qiagen) [20]. Carboxy-modified Qdots (2.8 nm, 522 nm), activated with EDC and Sulfo-NHS (Pierce), are covalently linked to ssDNA, chemically modified at the 5' end (Fig. 1) [21]. During the coupling reaction, Qdots are in 10-fold excess. Qdots which are not linked to ssDNA are removed by ethanol precipitation. Free Qdots are soluble in ethanol but Qdots link to DNA molecules precipitate. In the same way, uncharged gold nanoparticles (1.4 nm), functionalized with a single sulpho N-hydroxy-succinimide (NHS) ester (Nanoprobes) are covalently linked to ssDNA. As described above for the Qdot-ssDNA coupling, free Au particles are in excess and removed by ethanol precipitation. This method allows one to obtain, statistically, one emitter (or quencher) per ssDNA. Second, two complementary ssDNA, one attached to the Qdot emitter and the other attached to the metal quencher, readily self-assemble and form our Qdot-dsDNA-Au hybrid material [22].

The brightness of the Qdots and their photostability allow individual observations. Single-molecule studies yield a wealth of new information usually masked in

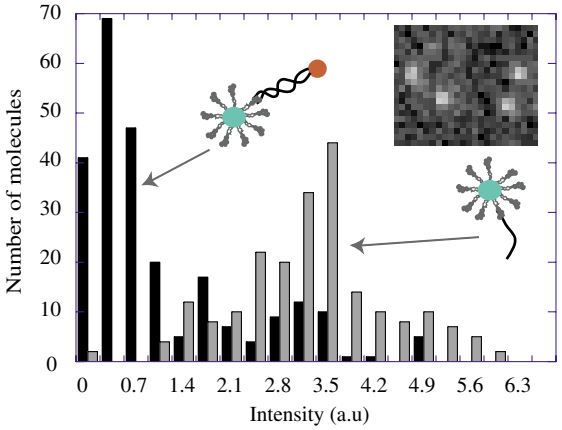

FIG. 1 (color online). Inset: Fluorescent observation of four Qdots adsorbed on a surface (acquisition time 500 ms). Histogram of the integrated intensity of individual Qdots and Qdot-dsDNA-Au complexes. The two measurements were performed successively and reported on the same plot. The gap between the Qdot-Au pair is 5.9 nm, which lead to a quenching efficiency of 82.3 ± 15.9%.

the ensemble-average signal taken from bulk measurements. We use dilute solutions of Qdots and Qdot-DNA-Au to visualize single emitters. The complexes are adsorbed nonspecifically to a clean cover slide and observed with an epifluorescent microscope. Images are acquired using a 100× oil immersion objective and a cooled CCD camera (SensiCam). Under continuous excitation, individual Qdots "blink": we observe a random switch between the fluorescent emission state of the particle and a "dark" state [8]. This fluorescence intermittency is characteristic of the observation of single and isolated fluorescent emitters.

After choosing a region of interest containing isolated emitters (Fig. 1, inset), we compute the integrated intensity of single Qdots (between 200 and 220 objects) and build a histogram of their intensity. This procedure requires careful subtraction of the fluorescence background. We measure successively the intensity of 2.8 nm individual Qdots and individual Qdot-dsDNA-Au complexes with an internanoparticle gap of seven base pairs. We obtain two distributions that we report on the same plot for convenience (Fig. 1). We can identify easily the two populations, which are separated in the intensity distribution. Thus, we can distinguish a population of unquenched Qdots from a population of partially quenched Qdots. One can extract, by fitting to a Gaussian distribution the histograms, the mean, and the distribution width for each population. We found an intensity ratio of 17% ± 9% between the partially quenched Qdots and the unquenched Qdot populations. From this ratio we estimate a quenching efficiency of 83% ± 9%.

The width of the intensity distribution is related in part to inherent single-molecule behavior. Three factors determine the distribution width: the heterogeneity of both emitters and quenchers, the shot noise, and the Qdot fluorescence intermittency. The heterogeneity of the emitters and quenchers is a consequence of the Qdot and Au size dispersion (~5%), the variation in particle shape, and the defects in crystals [23]. The shot noise is characteristic of low signal counts but the number of photons collected during the integration time (500 ms) is sufficient to reduce it to less than 3%. The third source of broadening of the distributions comes from the Qdot fluorescence intermittency. The random switch between emitting and nonemitting states is generally thought to be the result of Auger transient ionizations of the nanocrystals [8]: if two electron-hole pairs are created simultaneously in the crystal, the first pair recombination event powers the ejection of the electron or the hole from the second pair into a surface trap. In this case, the ionized Qdot is nonradiative and these events could be described as an intrinsic source of noise. Because of the broad range of time scales, which characterize the $1/f$ spectrum signature of the Qdot fluorescence, rare events of long duration dominate the signal. The duration of emitting states (or nonemitting states) of single Qdots are distributed according to a power-law distribution [24,25]. That particular distribution is characterized by a "long tail" which decays slowly with $t^{-(1+h)}$. When the exponent $h \in]0, 2[$ as it was determined for the Qdots, the variance is infinite. Thus, the fluctuations of the time averaged physi-

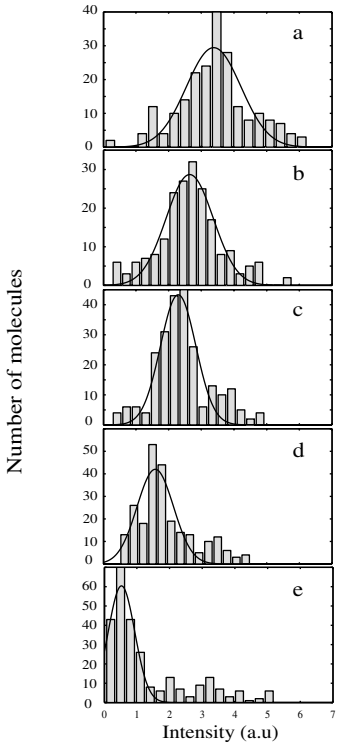

FIG. 2. Intensity distribution of single Qdot (top) and Qdot-dsDNA-Au complexes for, respectively, 7-11-15-21 bp DNA linker. The solid line corresponds to a Gaussian fit.

cal observables, like the integrated intensity of single Qdots, do not vanish even for long integration times. Whatever the integration time used for image acquisitions, we expect a significant part of the distribution width to come from the fluorescence intermittency.

We repeated the experiment for different DNA linker lengths: i.e., 7 to 21 bases. Four Qdot-dsDNA-Au complexes, of, respectively, 5.9, 7.3, 8.7, and 10.7 nm of interparticle distance, were constructed and studied. Results are reported in Fig. 2. The mean intensity shifts to lower intensity when the interparticle distance decreases. The largest intensity variations occur between the constructs 15 [Fig. 2(c)] and 11 bp [Fig. 2(d)] and between the constructs 11 [Fig. 2(d)] and 7 bp [Fig. 2(e)]. We extract the mean value and the width of each histogram by fitting to a Gaussian distribution. Figure 3 shows the quenching efficiency as a function of the spacer distance. The interparticle distance D is estimated to be the length of the dsDNA (3.4 Å per bp) plus the thickness of the micelle surrounding the Qdot (36 Å). The energy transfer decreases monotonically as the interparticle distance increases. This decrease is inversely proportional to the sixth power of distance and follows the curve of the Förster resonant energy transfer efficiency (solid line depicted in Fig. 3). This transfer is described by the function $1/[1 + (R/R_0)^6]$, where R_0, the Förster distance, is 7.5 nm [2]. The Qdot transient dipole, which has been observed for CdSe nanocrystals at room temperature [26], may induce a dipole in the gold particle. Within distances ranging from 5 to 10 nm, these two dipoles interact, leading to an energy transfer. This transfer is a nonradiative process between the Qdot (donor) and the gold (acceptor) and depends on both distance and relative orientation of the transient dipoles weakly coupled by long-range interactions. The dependence with the orientation between the emitter and the quencher disappear when the two nanoparticles are freely rotating on a time scale shorter than the fluorescence lifetime. Since the phospholipid layer surrounding the Qdot is a fluid phase, it can rotate inside the micelle under thermal agitation. Consequently, we expect an isotropy in the relative orientation of the dipoles.

In addition, we carry out an experiment to characterize the fluorescent emission properties of an ensemble of Qdot-Au complexes in solution. Measurements are performed using a spectrofluorimeter (PTI, NJ) at 20 °C with a 10 mm path length 100 μl cuvet (Starna Cells Inc). The integrated photoluminescence (PL) intensity of a solution of Qdots is calculated from the emission spectra. The PL is measured for three different samples (i) Qdot-ssDNA, (ii) Qdot-ssDNA and Au-ssDNA, with no complementarity between the ssDNA, and (iii) Qdot-DNA-Au complexes formed by hybridization between the two complementary ssDNA. The results for an interparticle distance of 5.9 nm are reported in Fig. 4 [27]. Assuming 100% efficiencies for both chemical conjugation and target hybridization, we estimate the quenching efficiency to be 67%. The 88% observed ratio between the experiments (ii) and (i) in Fig. 4 suggests a low level of nonspecific interactions as well as high recognition specificity of the complexes [28]. For larger gold particles only ($d > 2$ nm) the absorption spectrum exhibits a plasmon maximum at 520 nm [29]. The absence of plasmon peaks in the 1.4 nm absorption spectrum indicates that no clustering of nanoparticles occurs in our experiment. The bulk measurements for varying DNA linkers confirm the Förster-type behavior observed above (Fig. 3). Thus, we conclude that for distances larger than 5 nm a Förster-type process is involved between a CdSe nanocrystal and a gold nanoparticle. For short interparticle distances

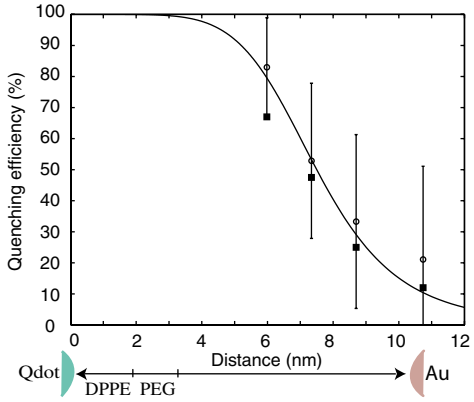

FIG. 3 (color online). Quenching efficiency as a function of the distance (circle: single-molecule studies; square: bulk measurements). The solid line corresponds to the resonant energy transfer function with $R_0 = 7.5$ nm. In the schematic DPPE represents the phospholipids and PEG, the polyethylene glycol, constituting the surrounding Qdot micelle.

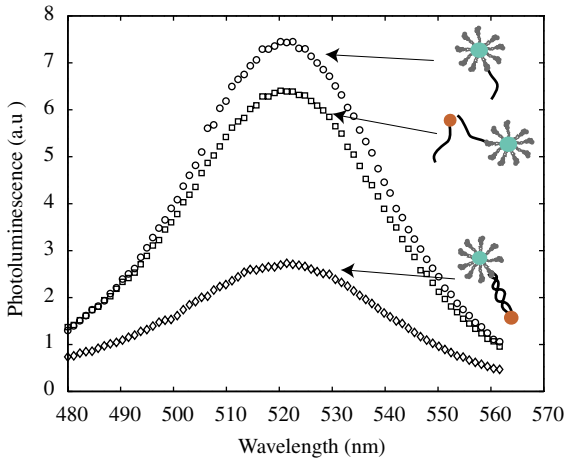

FIG. 4 (color online). Emission spectrum of a solution of ssDNA-Qdots (circle), a mixture ssDNA-Qdots and ssDNA-Au with no complementarity between the ssDNA (square), and Qdot-dsDNA-Au complexes (diamond).

($D < 5.5$ nm), and because of the DNA finite size, observations are difficult to obtain with our Qdot-dsDNA-Au construct. To overcome this difficulty, we directly link the gold nanoparticle to the Qdot without a DNA linker. For this construct, the gap between the emitter and the quencher is 3.6 nm and the transfer efficiency is 87% ± 5%, in agreement with the Förster prediction. At shorter distances other contributions may be considered. For example, electron transfer may give rise to additive nonradiative decay transfer between the CdSe nanocrystal and the metal surface [15].

We demonstrate that resonant energy transfer can be obtained by performing an analysis at the molecular scale. This, in turn, allows us to characterize the homogeneity of the sample studied and opens new perspectives for probing molecular interactions on bulk or on surfaces. Being able to measure the intermolecular distances between a single Qdot-Au pair might allow us to follow the conformational change of individual biomolecular assemblies.

We thank G. Bonnet, F. Vollmer, V. Noireaux, H. Salman, D. Braun, O. Ahmad, and L. LeGoff for enlightening discussions and suggestions. This investigation was supported by PHS Research Grant No. 5 R44 GM62100-03 from NIH-NIGMS. Z. G. thanks the FRM and Région Rhône Alpes for financial support.

*Corresponding author.
Electronic address: zoherg@rockefeller.edu

[1] S. Weiss, Science **283**, 1676 (1999).
[2] J. R. Lakowicz, *Principles of Fluorescence Spectroscopy* (Kluwer Academic/Plenum Publisher, New York, 1999).
[3] L. Stryer and R. P. Haugland, Proc. Natl. Acad. Sci. U.S.A. **58**, 719 (1967); T. Ha *et al.*, Proc. Natl. Acad. Sci. U.S.A. **93**, 6264 (1996).
[4] A. P. Alivisatos, Science **271**, 933 (1996).
[5] M. Jr. Bruchez, M. Moronne, P. Gin, S. Weiss, and A. P. Alivisatos, Science **281**, 2013 (1998).
[6] I. L. Medintz *et al.*, Nat. Mater. **2**, 630 (2003).
[7] V. I. Klimov *et al.*, Science **290**, 314 (2000).
[8] P. Michler *et al.*, Nature (London) **406**, 968 (2000).
[9] M. A. Hines and P. Guyot-Sionnest, J. Phys. Chem. **100**, 468 (1996).
[10] C. B. Murray, D. J. Norris, and M. G. Bawendi, J. Am. Chem. Soc. **115**, 8706 (1993).
[11] A. P. Alivisatos, Nat. Biotechnol. **22**, 47 (2004).
[12] C. F. Bohren and D. R. Huffman, *Absorption and Scattering of Light by Small Particles* (Wiley Science, New York, 1998).
[13] B. Dubertret, M. Calame, and A. Libchaber, Nat. Biotechnol. **19**, 365 (2001).
[14] H. Du, M. D. Disney, B. L. Miller, and T. D. Krauss, J. Am. Chem. Soc. **125**, 4012 (2003).
[15] E. Dulkeith *et al.*, Phys. Rev. Lett. **89**, 203002 (2002).
[16] N. C. Seeman, Nature (London) **421**, 427 (2003).
[17] Double-stranded DNA shorter than 150 bp can be considered as rigid molecules. A. A. Deniz *et al.*, Proc. Natl. Acad. Sci. U.S.A. **96**, 3670 (1999).
[18] A. P. Alivisatos *et al.*, Nature (London) **382**, 609 (1996).
[19] B. Dubertret *et al.*, Science **298**, 1759 (2002).
[20] Zucker's DNA mfold server was used to simulate conformation of oligonucleotides at room temperature. M. Zuker, Nucleic Acids Res. **31**, 3406 (2003). Four DNA sequences were chosen: 5' TTTGAGC 3', 5' TTTTGAGCGCG 3', 5' TTTTCCACATCCTCT 3', 5' TTTTGCTCAGTTCGAATGGAC 3'.
[21] G. T. Hermanson, *Bioconjugate Techniques* (Academic, San Diego, 1996).
[22] ssDNA-nanoparticles are mixed together (120 nm final) in a SSC buffer (1 ×) for 15 min at 38 °C and then left cooled at 20 °C for 105 min.
[23] Y. Ebenstein, T. Mokari, and U. Banin, Appl. Phys. Lett. **80**, 4033 (2002).
[24] K. T. Shimizu *et al.*, Phys. Rev. B **63**, 205316 (2001).
[25] X. Brokmann *et al.*, Phys. Rev. Lett. **90**, 120601 (2003).
[26] I. Chung, K. T. Shimizu, and M. G. Bawendi, Proc. Natl. Acad. Sci. U.S.A. **100**, 405 (2003).
[27] Tuning the excitation wavelengths (410 to 460 nm) does not change the general aspect of the emission spectrum. In the Fig. 4, the spectrum for a 430 nm excitation wavelength is reported. The ratio between the fluorescent intensity of the experiments (iii) and (ii), R , allows one to determine the quenching efficiency $P = (1 - R)$. In these experiments, we had systematically subtracted the fluorescent background by doing a measurement without qdots and gold. We idealized the hybridization scheme by assuming 100% efficiencies for both conjugation and target hybridization.
[28] The same results are observed with CdSe nanocrystals emitting at 546 nm.
[29] R. H. Doremus, J. Chem. Phys. **40**, 2389 (1964).